



Tropical cyclone multi-hazard risk mapping for Queensland, Australia

Cameron Do^{1,2,3} · Yuriy Kuleshov^{1,2,4}

Received: 21 July 2021 / Accepted: 20 January 2023 / Published online: 3 February 2023
© Crown 2023

Abstract

Tropical cyclones (TCs) are dangerous and destructive natural hazards that impact population, infrastructure, and the environment. TCs are multi-hazardous severe weather phenomena; they produce damaging winds, storm surges, and torrential rain that can lead to flooding. Identifying regions most at risk to TC impacts assists with improving preparedness and resilience of communities. This study presents results of TC multi-hazard risk assessment and mapping for Queensland (QLD), Australia. Datasets from Global Assessment Report (GAR) Atlas were used to evaluate TC hazards. Data for exposure and vulnerability of population, infrastructure and the environment were sourced from agencies such as the Australian Bureau of Statistics. TC hazards of storm surges, floods, and winds were analysed individually. Combining risk indices for TC hazards, exposure and vulnerability, overall TC risk index was derived. TC multi-hazard risk maps were produced at the Local Government Area level using ArcGIS, and regions with higher risk of being impacted by TCs were identified. The developed TC multi-hazard risk maps provide disaster risk management offices with comprehensive comparative TC risk profile of QLD that can be used to proactively manage TC risk at the subnational scale.

Keywords Tropical cyclones · Tropical cyclone risk · Hazards · Exposure and vulnerability · Multi-hazard risk mapping · Queensland · Australia

1 Introduction

1.1 Tropical cyclones

Tropical Cyclones (TCs) are dangerous and highly destructive natural hazards. Since 1970, almost 2000 natural disasters have been attributed to TCs, resulting in over 700,000 deaths

✉ Yuriy Kuleshov
yuriy.kuleshov@bom.gov.au

¹ Bureau of Meteorology, Docklands, VIC, Australia

² Royal Melbourne Institute of Technology (RMIT) University, Melbourne, VIC, Australia

³ Monash University, Clayton, VIC, Australia

⁴ The University of Melbourne, Parkville, VIC, Australia

and causing almost US\$ 1,500 billion in economic losses worldwide (WMO 2021). Australia, as well as many other nations in the tropics, is regularly affected by TCs. On average, 9 to 11 TCs occur in the Australian region each season, four of which typically cross the coast (Kuleshov et al. 2010; BoM 2020). Consequences of TC landfall are often disastrous, causing fatalities among the Australian population, damage to infrastructure and the environment, and negatively impacting the economy. From 1967 to 1993, the insurance payout of TCs and severe thunderstorms in Australia have totalled to over US\$ 1.2 billion each and resulted in the loss of 4 to 6 lives each year (Ryan 1993). One of the recent examples is an impact of TC *Debbie* on Australian states of Queensland (QLD) and New South Wales in 2017. *Debbie* caused fourteen deaths across Australia, primarily as a result of extreme flooding, and US\$ 2.75 billion in damage (Cyclone Debbie 2017). It was the deadliest TC since TC *Fifi* in 1991 which killed 29 people. *Debbie* was the second costliest TC cyclone in Australia since TC *Yasi* in 2011 which caused damage of about US\$ 3.6 billion. These recent TC impacts reinforce importance of further improving TC risk assessments and strengthening TC early warning systems.

The main hazards associated with TCs are destructive winds, storm surges and torrential rain potentially resulting in flooding and / or landslides. As well as affecting regions differently, impacts of TC hazards can compound to cause even greater damage (Gori et al. 2020). The impacts of storm surges and flooding contribute the most damage to population, infrastructure and the environment (Mendelsohn and Zheng 2020; Zhang et al. 2008).

To improve preparedness and strengthen resilience of communities at risk, advanced methods for TC seasonal forecasting for the Australian region have been developed (Wijnands et al. 2015; Qian et al. 2022) and TC early warnings are disseminated operationally (Kuleshov et al. 2020). However, existing forecast and warning tools place emphasis on wind speed in estimating TC intensity and category (Lavender and McBride 2020). This could be particularly problematic when users may need to understand the diverse range of risks TCs pose through interpretation of wind-based risk warnings alone. For example, storm surge height cannot be inferred from wind intensity warnings as surge magnitude is not linearly related to TC intensity (Mortlock et al. 2018).

Accounting for the multi-hazard nature of TC risk is a challenge, and a standardised approach has not been developed yet (Anderson et al. 2020). This study addresses the complexity of TC risk assessment by mapping TC hazards individually and then combining hazards with exposure and vulnerability to estimate overall TC risk. This proof of concept methodology is an attempt to contribute towards the long-term goal of developing standardised multi-hazard TC risk analysis.

1.2 Risk analysis

For the purpose of this study, the following definitions of hazard, exposure, vulnerability and risk are used (Crichton 1999; Downing et al. 2001):

- Hazard: the probability of the hazard event occurring and its intensity;
- Exposure: the population, infrastructure and environment within the hazard's extent;
- Vulnerability: the susceptibility of people, infrastructure or the environment to be damaged by the event measured by physical and social factors, taking into consideration their coping capacity and preventive measures;
- Risk: the probability of harmful consequences, or expected losses resulting from interactions between hazard, exposure and vulnerability.

Risk assessments are critical for identifying highly exposed and most vulnerable regions that are priority for efficient disaster management (Aguirre-Ayerbe et al. 2018; Ahmed 2020). Risk assessments combine hazard information with data on human activity, infrastructure and natural resources to determine possible impacts of hazardous events (National Research Council 1991). Risk assessments allow individuals, businesses, communities, and governments to make informed decisions for risk management. With climate change altering the environment, and the evolving nature of human activity, risk assessments must likewise be updated to stay useful and relevant as a disaster risk reduction tool.

Comprehensive TC hazard assessments have been predominantly conducted for small scale regions such as coastal towns or cities (Churchill et al. 2017; Hoque et al. 2017; Sahoo and Bhaskaran 2018). The limiting factor is the need to run hazard models over the study area using high resolution input data (e.g., topography and bathymetry) which is computationally expensive to do over large regional domains (Lee et al. 2018). Extending studies from hazard assessments to risk assessments additionally requires substantial exposure and vulnerability data which is available for Australia from agencies such as the Australian Bureau of Statistics (ABS). This information is commonly collected at lower resolution levels of Local Government Areas (LGAs) or Statistical Area level 1 (SA1) regions. Thus, regional risk assessments are often restrained by unavailability of high resolution exposure and vulnerability data, as well as the lack of region-specific high resolution hazard model outputs.

1.3 Hazard models

A number of TC hazard models exist, ranging from statistical modelling to numerical, probabilistic, dynamical and ensemble predictions (Hoque et al. 2017, Mohanty and Gupta 1997). For case studies of single-storm events, deterministic models are often used for research and model improvement purposes. Deterministic predictive models require accurate meteorological inputs such as TC position, pressure, wind speed and timing which is achievable in hindcasting a TC post-occurrence (Moskaitis 2008).

Ensemble and probabilistic models are used to predict the chance certain hazard intensities will occur for certain return periods. Using historical TC track data, these models simulate similar storm events thousands of times, to obtain outputs which describe TC-related hazards, e.g., predicted 2 m storm surge height for a 100-year return period (Volpi et al. 2015). For different TC hazards of storm surge, flooding and wind, different inputs are required, and often of high resolution. In absence of readily available region-specific high resolution hazard model outputs, lower resolution global datasets (Cardona et al. 2014; Muis et al. 2016; Plotkin et al. 2019) can be used for TC risk assessment.

1.4 TC risk assessment in Australia

Assessing TC hazard, exposure, vulnerability, and risk in Australia, most of earlier studies were focused on examining one hazard (Arthur 2021; Rygel et al. 2006; Paerl et al. 2020). In addition, barriers still exist in data sharing between academia, industry, and government within the field of natural hazard risk in Australia (Haynes et al. 2017; Mortlock et al. 2018). State resources have been put into producing generalised risk assessments for natural hazards, e.g., the ‘Queensland State Natural Hazard Risk Assessment 2017’. Such assessments have useful descriptions of which sectors and industries are exposed or

possibly impacted; however, no quantifications or region-specific information follows to enable stakeholders to take action.

Risk assessments, together with early warning systems and post disaster reviews, are key components of proactive disaster management (Bhardwaj et al. 2021). Early warning systems are used to monitor, predict, and communicate TC threats to communities at risk. In Australia, the Bureau of Meteorology (BoM) is tasked with the responsibility of monitoring and issuing warnings for TCs as part of the Meteorology Act (1955). At shorter time scales, statements of TC watch or warning are given within 48 h of expected gale force winds (63 km/h). At longer time scales, seasonal TC outlook is issued prior to the start of TC season (in the Southern Hemisphere, TC season is typically from November to April; see Kuleshov (2020) for detail).

All components of proactive disaster management are interconnected, e.g., risk assessments provide vital information which is used to determine priority regions for implementing or further strengthening early warning systems. Hence, by improving TC risk assessments, there exists the opportunity to improve longer term TC risk information and build resilience in regions most exposed to TC risks.

While an earlier study by Do et al. (2022) assessed TC risk to Australian coral reefs using wind model data, this study presents TC multi-hazard risk mapping for QLD, Australia considering the effects of storm surges and TC-induced flooding alongside winds. The paper is organised as follows. Section 2 describes data and methodology used for TC multi-hazard risk assessment. Results of TC risk mapping for QLD and a case study for TC *Debbie* are presented and discussed in Sect. 3. Conclusions are presented in Sect. 4.

2 Data and methodology

2.1 Study area

Map of study area with QLD LGA divisions is presented in Fig. 1; a map of QLD with named LGA regions can be found in Appendix 1.

For TC risk mapping, QLD was divided into LGAs as the base resolution for this study to best suit datasets available. This involved joining data into polygon shapefiles of QLD LGAs. Data were collated and mapped using ArcGIS Pro.

Risk mapping is a form of risk assessment that visualises the components of risk as hazard, exposure, and vulnerability layers on a map. This can further be broken down into inputs of hazard (e.g., winds, floods, storm surges), indicators of exposure (e.g., population density), and indicators of vulnerability (e.g., socio-economic disadvantage). The conceptual framework used in this study for TC Risk index calculation and subsequent mapping based on three levels of products is presented in Fig. 2.

Risk maps are often choropleth, meaning regions are thematically coloured according to chosen characteristics, and are displayed with classes from very low/no risk to very high risk. Spatial resolution of risk maps is often quite low, as it is constrained by the resolution of available inputs, e.g., vulnerability data at the LGA or SA1 level.

2.2 TC exposure index

To represent the exposure of assets, i.e., population, infrastructure, and the environment, one indicator was selected for each category, namely population density, amount



Fig. 1 Map of study area with QLD Local Government Area divisions. A regional inset is included

of critical infrastructure and coral area. Population density is commonly used as an indicator of human population exposure in similar studies (Sahoo and Bhaskaran 2018; Amadio et al. 2019); however, the inclusion of infrastructural and environmental exposure is less common. For infrastructure, a proxy was created from a dataset of critical infrastructure shapefiles, which included hospitals and emergency service buildings. It was assumed that the loss of this critical infrastructure would lead to significant impact, and that a higher value suggested the LGA had more infrastructure exposed overall. For environmental exposure, coral area was calculated from the Great Barrier Reef (GBR) feature polygons, and areas of corals were summed for LGAs based on their ocean boundaries. While past studies have explored the impacts of TCs on coral reef environments and identified their value in reducing flood and surge impacts (Puotinen et al. 2020; Beck et al. 2018), this study is the first to include corals as valuable assets exposed alongside population and infrastructure.

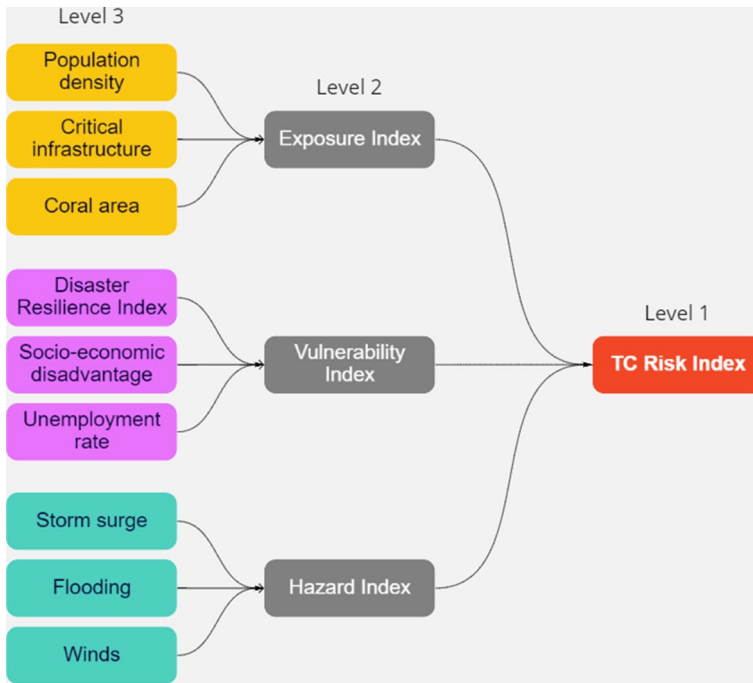


Fig. 2 Three levels of products for TC risk assessment and mapping

2.3 TC vulnerability index

Vulnerability indicators should be specifically selected to be most applicable for the study area (Sahana et al. 2019). This study used the Australian Disaster Resilience Index (DRI), Index of Relative Socio-economic Disadvantage (IRSD), and unemployment rate, where higher DRI inverse, higher IRSD and higher unemployment rate indicated higher vulnerability. The DRI was a highly relevant and robust indicator selected as it directly relates natural hazards and the resilience of regions. It was developed by the Bushfire and Natural Hazards Cooperative Research Centre (BNHCRC) and included the calculation of 75 indicators for coping capacity and adaptive capacity (BNHCRC 2020). As DRI data were presented at SA1 level, for this study, we averaged them to represent vulnerability at LGA level. IRSD and unemployment rate have been used in past risk and vulnerability assessments (Ntajal et al. 2016; Rolfe et al. 2020), and are available for Australia from the Australian Bureau of Statistics (ABS).

Summary of datasets used as inputs for calculating TC Exposure and TC Vulnerability Indices and the data source is presented in Table 1.

2.4 TC hazard indices

Probabilistic hazard model data for storm surges, floods, and winds was sourced from the Global Assessment Report (GAR) Atlas (2015). The 100-year return period was selected

Table 1 Summary of datasets used for calculating TC Exposure and TC Vulnerability Indices and their source

Indicators	Dataset used	Source	Year	License
<i>Exposure</i>				
Population density	Estimated resident population by LGA	ABS	2011	Creative Commons CC BY-NC 4.0 licence
Critical infrastructure	Critical infrastructure (hospitals, emergency service buildings, etc.)	Queensland QSpatial	2021	Creative Commons—Attribution 4.0 International licence
Coral area	Great Barrier Reef features	GBR MPA geoportal	2019	Creative Commons—Attribution 4.0 International licence
<i>Vulnerability</i>				
Disaster resilience	Disaster Resilience Index	BNHCRC	2020	Creative Commons CC BY-NC 4.0 licence
Unemployment	Unemployment rate by LGA	ABS	2011	Creative Commons CC BY-NC 4.0 licence
Socio-economic disadvantage	SEIFA's IRSD	ABS	2016	Creative Commons CC BY-NC 4.0 licence

for all three hazard datasets as it is commonly used to analyse TC hazard risk (Didier et al. 2018). The storm surge dataset provided numerous surge height values along the QLD coast. To obtain one surge hazard value per LGA, the mean surge height (m) was calculated in ArcGIS Pro using Spatial Join. The wind dataset was in raster form and using Raster to Polygon, again cell values were averaged within each LGA using Spatial Join. The riverine flood dataset had high values distributed around inland water catchments and basins and considered regular flood rather than TC-induced flood. To adjust the dataset to incorporate the effect of TCs, flood raster values were multiplied by values from the wind dataset with Raster Overlay, which emphasised flood hazard towards the north-east direction where most QLD TCs originate. Cell values were then summed per LGA instead of averaged to account for the fact that most raster values within LGAs were null. Thus, higher flood hazard LGAs are those with more rivers/water bodies rather than those with one high value.

2.5 TC risk indices

Data for exposure and vulnerability indicators as well as hazard values were normalised into values from 0 to 1 except the DRI and IRSD which already standardised. Inverse values were taken for some indicators, e.g., DRI, as a lower DRI indicates a region is more vulnerable to a natural hazard.

Calculating exposure and vulnerability indices, an equal weighting for each indicator was used. Creating a weighted framework was out of the scope of this study given little literature exists specifically for TC risk assessment in Australia.

Following recommendations for modelling TC risks using geospatial techniques (Hoque et al. 2017), risk was calculated using the Eq. 1:

$$\text{Risk} = \text{Hazard} \times \text{Exposure} \times \text{Vulnerability} \quad (1)$$

3 Results and discussion

To evaluate performance of the developed TC multi-hazard risk assessment and mapping methodology, we first examined a case study of TC *Debbie* which recently caused death and damage in QLD.

3.1 Case study: TC *Debbie*

For the case study of TC *Debbie* (2017), historical data from the Southern Hemisphere TC archive (Kuleshov 2020) was used and buffers were created around cyclone's path. Classes of hazard risk were assigned from low (0.2) to high (0.8) based on distance from the TC centre. Additionally, news and weather reports of hazard damage were used to confirm assigned classes. As the three TC hazards differ in extent and damage, different sized buffers were used. For example, a 200 km buffer was used for the highest class of flood hazard whereas for storm surges and winds buffers of 100 km and 50 km were selected, respectively. These buffer values were arbitrarily chosen based on relative extent and magnitude of impacts. Additionally, all inland LGAs were given a class value of 0 for storm surges to ensure that end risk calculations accurately equalled 0.

3.1.1 TC exposure index

To calculate TC Exposure Index at LGA level, three indicators which represent TC exposure to assets of population, infrastructure, and environment were selected, namely population density, critical infrastructure, and coral area, which were then combined using equal weighting (Fig. 3).

Low values of population exposure (less than 0.16) throughout QLD LGAs were found, with the exception of regions surrounding the capital city of Brisbane which has the highest value (Fig. 3a). Infrastructure exposure map reveals higher values again around Brisbane, but also along the eastern coast and further inland (Fig. 3b). Coral exposure is evident for coastal LGAs within the extent of the GBR; Cook Shire, a large northern LGA with the largest oceanic bounds, has the highest value of 1 (Fig. 3c). Most LGAs inland from the north-eastern coastline have low population densities, less infrastructure and understandably no associated coral exposure.

The resultant TC Exposure Index map shows high exposure values for the Cook Shire, Brisbane, and surrounding regions, as well as moderate values for LGAs in the eastern to south-eastern parts of QLD (Fig. 3d). The prevalent transition tendency from high level of exposure for coastal LGAs to low exposure levels for western and south-western inland LGAs is consistent for all three selected indicators and the resultant TC Exposure Index.

Similarities between the population and infrastructure indicators around Brisbane suggest a correlation between population density and number of critical infrastructure buildings. This correlation is commonly accepted as infrastructure is built to address needs of population. For critical infrastructure in particular, emergency service buildings are placed to cater for a portion of the region and their population, with, for example, hospitals housing 4 beds per 1,000 citizens in Australia (Wilson et al. 2010). Despite this correlation between the indicators shown primarily through high values for densely populated Brisbane and surrounding regions, similarities are not obvious for the rest of the LGAs other than a few regions near the coast.

For the number of critical infrastructure buildings, values ranged from 0 to 117 buildings per LGA. This was calculated by counting the number of hospitals and other emergency service buildings in each LGA in ArcGIS. The next step was normalisation using the equation $(x - \min) / (\max - \min)$, which places the lowest value at 0 and highest at 1. Using this method on a distribution of population data with one very high value (e.g., Brisbane: 930 persons/km²), the rest of the values are expected to be much lower in comparison. For example, the next highest population density value is Gold Coast City with 465 persons/km², which after normalisation equated to ~0.5. The other 77 LGAs yielded post-normalisation values between 0 and 0.5. Comparing this to number of critical infrastructure buildings, Brisbane had 117 (value of 1 post-normalisation), followed by Toowoomba Regional with 78 (0.67) and Gold Coast City with 73 (0.62).

The limitation of normalisation is that outliers can largely increase the range and lower all other values. For a dataset of population density with the capital city of Brisbane as an outlier, this causes the more rural LGAs to be represented with near-zero values. Further study could implement capping outliers to reduce the range or ranking systems that groups raw data values into deciles, where, for example, the highest 10% of LGAs are assigned a value of 1. Alternatively, other normalisation methods such as ArcTan S-function normalisation could be used to reduce the weight of values at the extremes (Den Boer 2011).

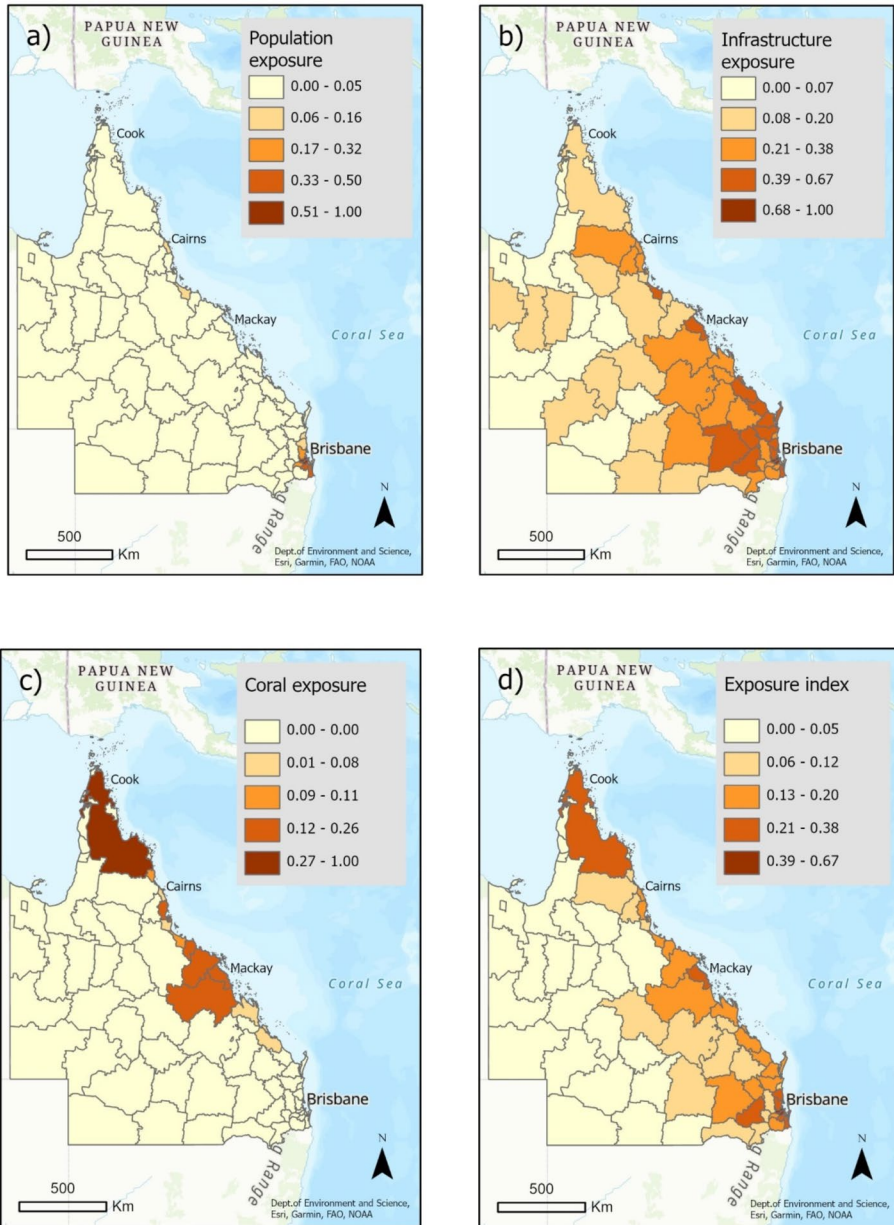


Fig. 3 Maps of TC Exposure indicators: **a** population density, **b** critical infrastructure, and **c** coral area, which were used to calculate TC Exposure Index at LGA level **d**

3.1.2 TC Vulnerability index

The three indicators DRI inverse, IRSD and unemployment rate were equally weighted to calculate TC Vulnerability Index. Results indicate low disaster resilience and hence high

vulnerability in the north-western LGAs according to DRI inverse values (Fig. 4a). This is also seen with higher classes of socio-economic disadvantage in the north-west as well as areas of higher disadvantage in the regions north of Brisbane (Fig. 4b). Unemployment rate is at a low level for most LGAs (Fig. 4c). Combining these three indicators together, the

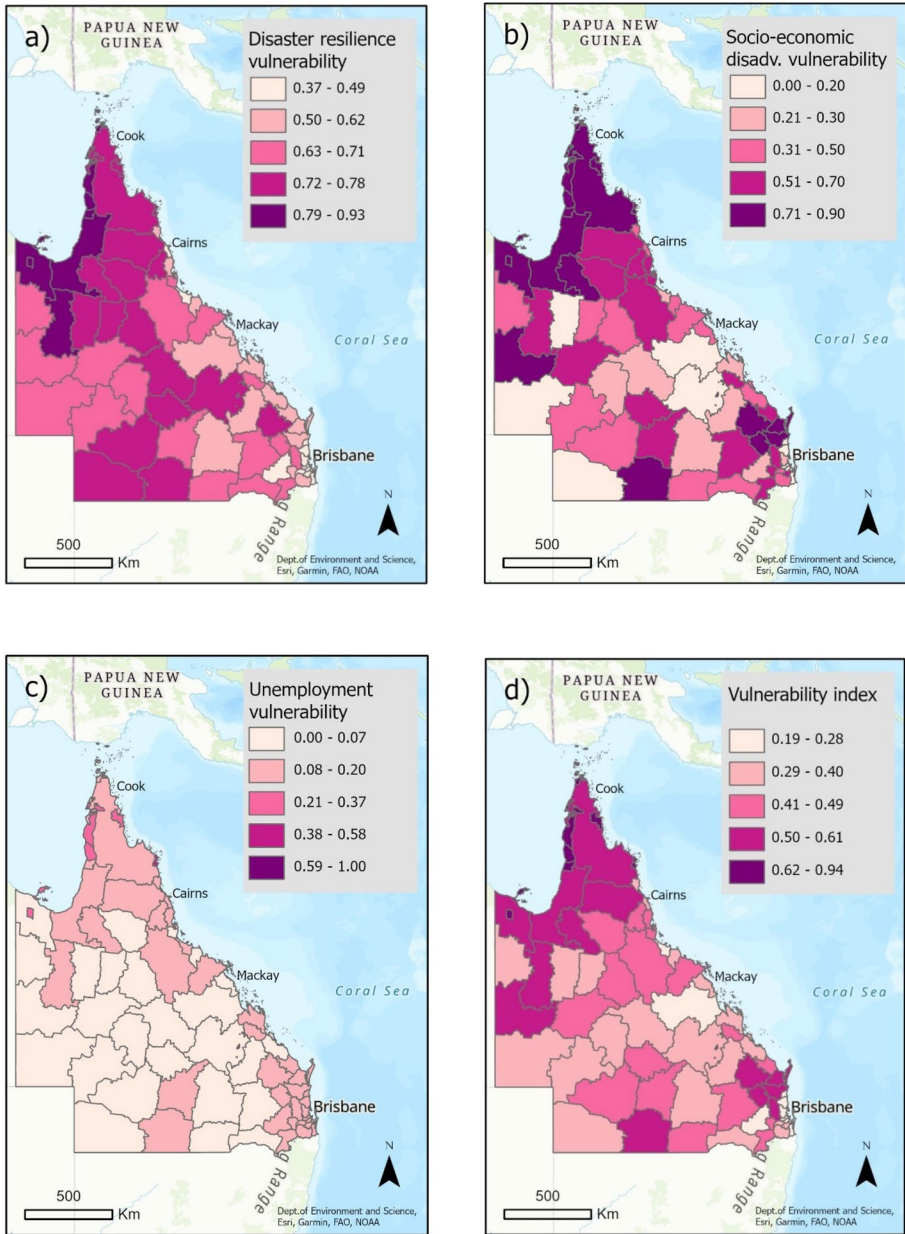


Fig. 4 Maps of LGA vulnerability using indicators of **a** DRI inverse, **b** IRSD, and **c** unemployment rate, used to calculate TC Vulnerability Index (**d**)

final TC Vulnerability Index map shows highly vulnerable regions in northern and north-western QLD, as well as in the LGAs north of Brisbane (Fig. 4d). Note that Brisbane and surrounding LGAs are classed with the lowest to second lowest vulnerability. Additionally, due to the unemployment rate having relatively similar values throughout the state, this indicator has little impact on the overall TC Vulnerability Index.

The similarities of DRI inverse and IRSD could be explained by the fact the DRI was created using a large number of indicators, some of which could overlap with socio-economic disadvantage. This could lead to an overestimation or overvaluing of socio-economic disadvantage as an indicator. Compared to other indicators used in this study to assess vulnerability which have been chosen for data availability and convenient access, the DRI indicator was the most robust and relevant indicator.

The assumed confidence in particular indicators used in this study versus others suggests that a weighted framework to calculate indices would improve accuracy of results. For example, rather than equally weighting the three indicators by adding them together with 1/3 multipliers, a more robust indicator could be weighted higher with a 1/2 multiplier while the remaining two indicators each have 1/4 multipliers. This would ensure the more robust indicator has a higher influence on end risk maps, and at the same time reduce the effects of indicators we are less confident in. Weighted frameworks for index creation are often subjective; however, and extensive specific research would be needed to create weighting systems that are justified (Amadio et al. 2019). This was out of the scope of this proof-of-concept study.

All three selected indicators to assess TC vulnerability are related to the potential TC impacts on the human population. Calculating overall TC Risk Index, TC Vulnerability Index which is solely based on population vulnerability is combined with TC Exposure Index which is comprised of inputs related to population, infrastructure, and the environment. In the context of this study, population vulnerability indicators were solely used because of data availability. While potential vulnerability indicators in the form of building code/strength for infrastructure exposure, or coral health for the environment may be able to be derived, the data did not yet exist to create a robust index.

3.1.3 TC hazard index

Hazard maps of TC *Debbie* are presented in Fig. 5. Storm surges represent a hazard for all coastal LGAs throughout QLD, with highest hazard level at coastal LGAs around Mackay – an area of TC *Debbie*'s landfall (Fig. 5a). Flood hazard extends far inland affecting over 80% (65 out of 78) of QLD LGAs (Fig. 5b). In contrast, wind hazard is relatively confined to LGAs along the path of TC *Debbie* (Fig. 5c).

All three hazard maps clearly demonstrate the highest level of hazards along the path of TC *Debbie*. Evaluating level of hazards during our post disaster review, we used TC *Debbie* best track data to create buffers, and we also used reports of surge height, flooding, and wind speed at different LGAs to calibrate the buffer radius and class values. It is important to estimate risk from each hazard individually, as damage which they cause to population, infrastructure, and the environment differs. For example, winds may uproot trees and damage buildings whereas flooding and storm surge inundation can disrupt nutrient balances in soil and water, while also flooding buildings and potentially drowning humans, livestock, and wild animals.

Flooding typically has the greatest areal extent compared to other hazards due to wider impact of torrential rain during the system's TC stage and after its weakening into a low

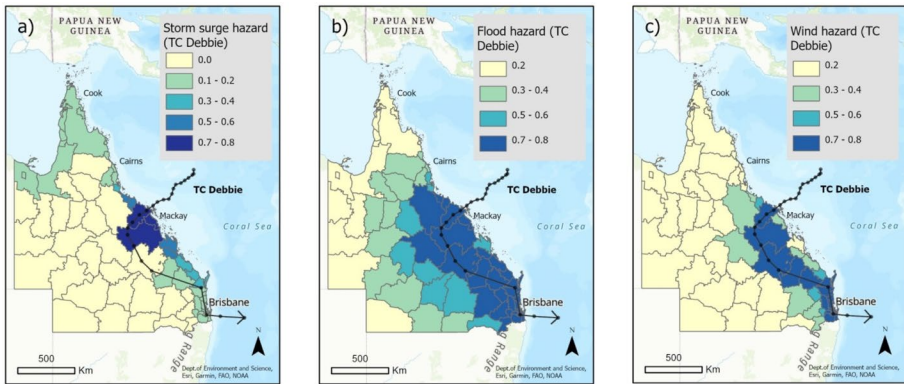


Fig. 5 Maps of TC hazards for QLD LGAs: **a** storm surges, **b** floods, and **c** winds; case study for TC *Debbie*

pressure system (Touma et al. 2019); case study for TC *Debbie* confirms this earlier finding.

Storm surge affected LGAs near the coast, with highest level of hazard in the vicinity of TC landfall. All coastal LGAs have greater than zero storm surge values as 0.2 was initially chosen as the lowest class in line with wind and flood hazards, with the understanding TCs may have wider impacts on surrounding atmospheric and ocean circulations.

Wind buffers were chosen with maximum hazard level for LGAs where their centres were within a 50 km buffer of the TC path, in accordance to the ‘most destructive path’ (Hsu and Yan 1998; Bhardwaj et al. 2021). The weakening of TC *Debbie* over land was not accounted for in wind or flood hazards however, which should be considered when examining hazard risk maps (Sect. 3.1.4).

Hazard values were given four classes with equally spaced values of 0.2, 0.4, 0.6 and 0.8. For storm surge specifically, an additional fifth class was added with a value of 0 for far inland LGAs where storm surge hazard does not exist. This 0-value class was not included for wind and flood hazards as the low-pressure systems and TCs can have effects at large distances depending on their size. These equally spaced hazard values were arbitrarily given and not based on specific hazard measurements such as surge height, wind speeds or inundation depths.

An alternative approach to assign classes of hazard would be based on the possible damage caused, for example with 0.1 equating to where winds reached certain predefined threshold, e.g., gale force winds when wind actions result in damaging buildings (Structural design actions Part 2: Wind actions 2011). For this case study, a simpler approach was used to show an effective proof of concept that may be expanded in the future using complex wind speed models (Wijnands et al. 2016).

3.1.4 TC risk indices—TC *Debbie*

TC Risk Indices for storm surges, floods and winds were produced by multiplying TC Exposure Index, TC Vulnerability Index and TC Hazard Index for the respective hazard (Eq. 1). Overall TC Risk Index was calculated by equally weighting risk indices of all three hazards. Maps of the three risks (storm surges, floods, and winds) and overall TC

risk associated with TC *Debbie* were generated using ArcGIS (Fig. 6). The maps clearly demonstrate that TC risk is high over LGAs along the QLD eastern coast and within the path of TC *Debbie*. For storm surge risk (Fig. 6a), mostly coastal LGAs have higher risk in comparison to flood risk (Fig. 6b) and wind risk (Fig. 6c).

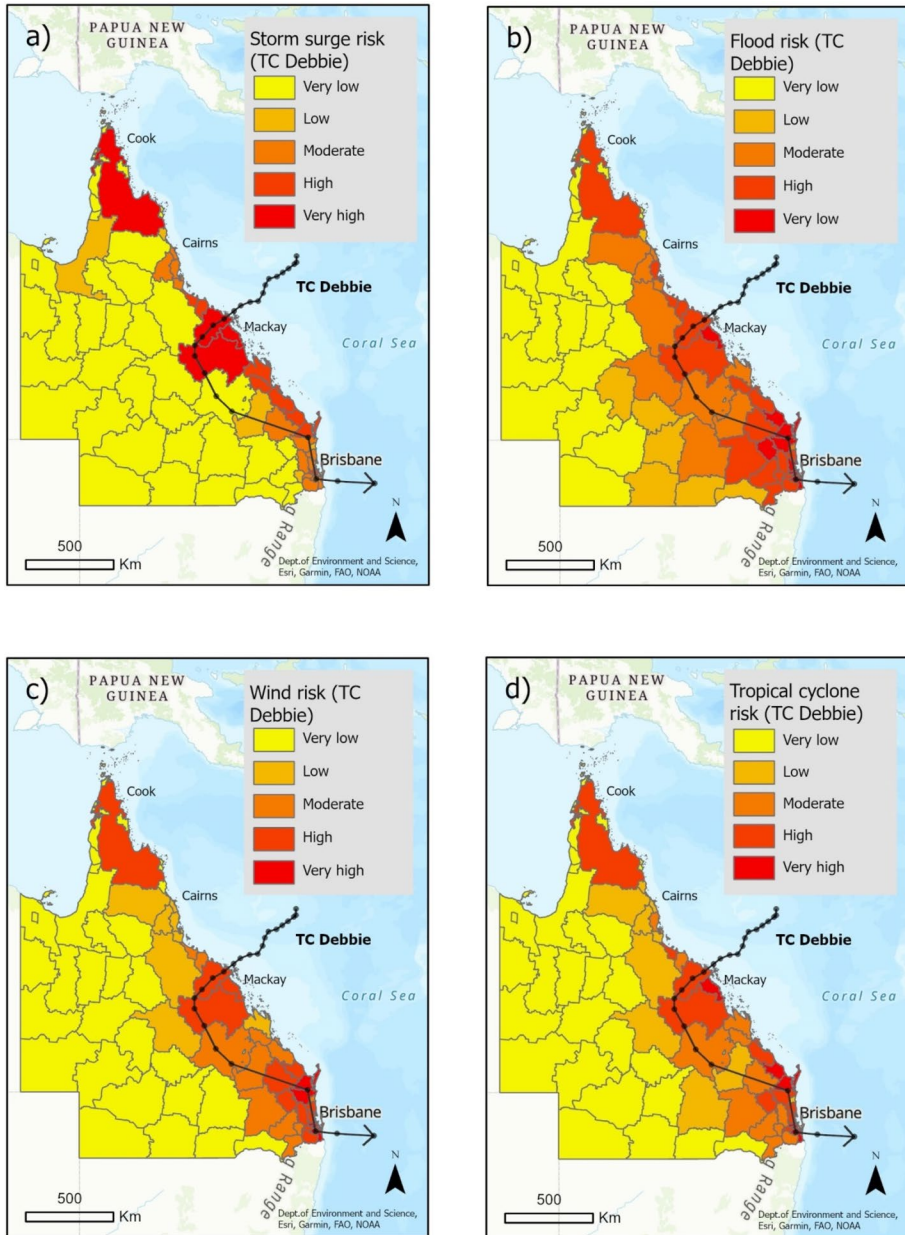


Fig. 6 Maps of TC Risk for QLD LGAs: **a** storm surges, **b** floods, **c** winds, and **d** a combined TC Risk map produced by averaging risk from all three hazards; case study for TC *Debbie*

One consistently high risk area is Cook Shire in far north QLD that is classed as ‘very high’ risk for all three hazards, despite being located far from the path of TC *Debbie*. Cook Shire’s consistently high risk can be explained by the region’s high exposure and vulnerability index values, which when multiplied by low hazard factors of 0.2 to 0.4 still results in a very high risk value in comparison to the rest of the state. This result suggests hazard values for LGAs far from TC track need to be lowered and identifies the need for more accurate model-driven data to create hazard layers.

Another observation is that for flood and wind risk, LGAs around Brisbane have higher risk than some LGAs that are also within the path of TC *Debbie*. This can be explained by Brisbane and its surrounding region having a higher exposure with more population and infrastructure at risk.

A case study for TC *Debbie* demonstrates usefulness of the designed methodology for assessing risk at various levels for an individual TC event. However, a constraint of this study is the lack of region-specific post-disaster spatial data, which could be used to validate hazard and risk maps. A lack of a standardised approach to selecting exposure and vulnerability indicators also influenced the results, along with choice of indicators for TC risk assessment. Similarly, proxies such as number of critical infrastructure buildings may not be most representative for evaluating exposed infrastructure per LGA. Additionally, while natural breaks classification is valuable for mapping, the same class from each risk layer would not be equivalent. For example, very high flood risk would not equal the same risk of damage as very high wind risk. Such inconsistencies, while minor, can be addressed in future research and through additional validation of results obtained in this study.

3.2 TC risk mapping for Queensland

TC risk assessment and mapping is a valuable decision-support tool for improving preparedness to this natural hazard and further strengthening proactive disaster management, e.g., timely evacuation of population at risk, emergency response and future planning (Kuleshov et al., 2009a; Dube et al. 2010). Using global hazard model data from the GAR Atlas data platform, TC hazard maps for QLD have been created (Fig. 7).

Examining distribution of TC wind hazard over QLD, one can see the highest values for LGAs located on the eastern coast and their gradual decrease for LGAs to the south-west

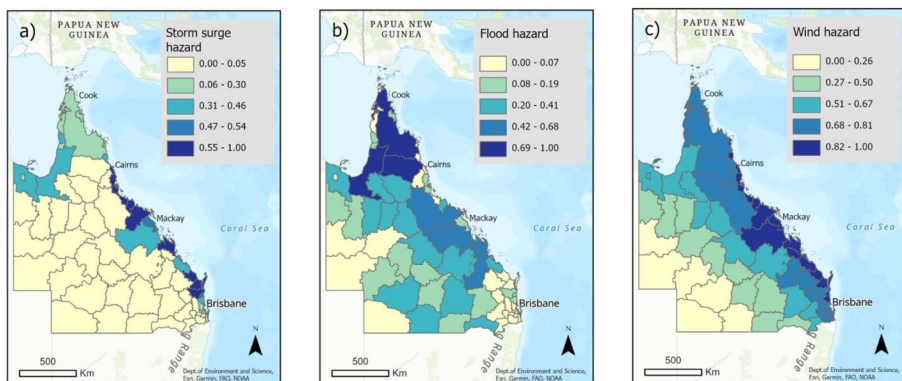


Fig. 7 Maps of TC hazards for QLD LGAs: **a** storm surges, **b** floods, and **c** winds

inland (Fig. 7c). This is related to the weakening of TC intensity when cyclones are moving over land as there is no source of thermal energy from warm oceanic water for their development (Gray 1988; Kuleshov et al. 2008, 2009b; Colette et al. 2010). For storm surges (Fig. 7a), hazard level is also higher on the eastern coast, however compared to wind, the highest hazard class is not observed consistently. This suggests that eastern coast LGAs with lower level of storm surge hazard have topography and bathymetry that reduces the probability of high storm surge. Map of flood hazard (Fig. 7b) shows the highest level of hazard for large LGAs in northern QLD. Generally, LGAs to the north-east have higher flood hazard, excluding LGAs smaller in size. This can be explained by mapping methods used that overlay the original riverine flood dataset with the wind hazard data to derive TC-induced flood, which explains higher values to the north-east. Smaller LGAs generally had very low flood hazard scores as when converting from raster to polygon, flood inundation values were summed per LGA, meaning larger LGAs were more likely to have more raster cells with flood values. This indicates that LGAs with higher values have more riverine/lake features that are at risk of flooding and are closer to the expected path of TCs.

Combining model-derived TC hazard indices with the derived TC Exposure and TC Vulnerability Indices, TC Risk Indices were calculated using Eq. 1, and TC Risk maps for each hazard were produced (Figs. 8a-d).

Regions in northern and north-western QLD, as well as south-eastern QLD north of Brisbane, were identified as most exposed and vulnerable to TC impacts (Figs. 3d and 4d, respectively). Thus, it is expected for those regions to also have high level of TC risk especially considering strong impact of all three hazards on LGAs at the eastern coast (Figs. 7a-c).

For storm surges (Fig. 8a), most of the eastern coast LGAs are at very high or high level of risk, and the north-western coastal regions have very low risk. For flood risk (Fig. 8b), distribution resembles the flood hazard map (Fig. 7b), with LGAs at the highest risk along the eastern coastline, and low to moderate risk levels for LGAs further inland. Despite higher exposure along the coastal LGA's, smaller LGAs particularly south of Cairns are classed with very low to low flood risk. The wind risk map (Fig. 8c) shows very low risk for inland western and central QLD, and high to low risk for LGAs along the eastern coast. Note that Cook Shire has very high wind risk, which is seen to be the case for other hazards as well.

The overall TC Risk map produced by averaging risk values of storm surge, flood, and wind hazards is presented in Fig. 8d. A few regions of higher risk are identified: Cook Shire in the north, a group of LGAs surrounding Mackay Regional, and the region north of Brisbane including Gympie and Fraser Coast Regional LGAs.

The TC risk maps produced from model-derived hazard data are informative and novel for the study region. By knowing TC risk, more efficient actions can be taken to reduce potential negative impacts. As the different hazards of TCs impact communities and the environment differently, having risk maps for each hazard individually can prevent miscommunication and mistrust of authorities which are known to greatly inhibit decisive action (Garcia and Fearnley 2012). As shown in Fig. 8, the extent and severity of risks associated with TCs depends on the hazard, and this study contributes to visualising their multi-hazard nature.

This study is a proof-of-concept to demonstrate value of TC multi-hazard risk assessment and mapping, and we will continue to refine the methodology in our future research. As the overall TC Risk layer is calculated by multiplying values of exposure, vulnerability and hazard, errors and constraints from previous layers persist. Without thorough validation of the accuracy of maps based on past event data and post disaster

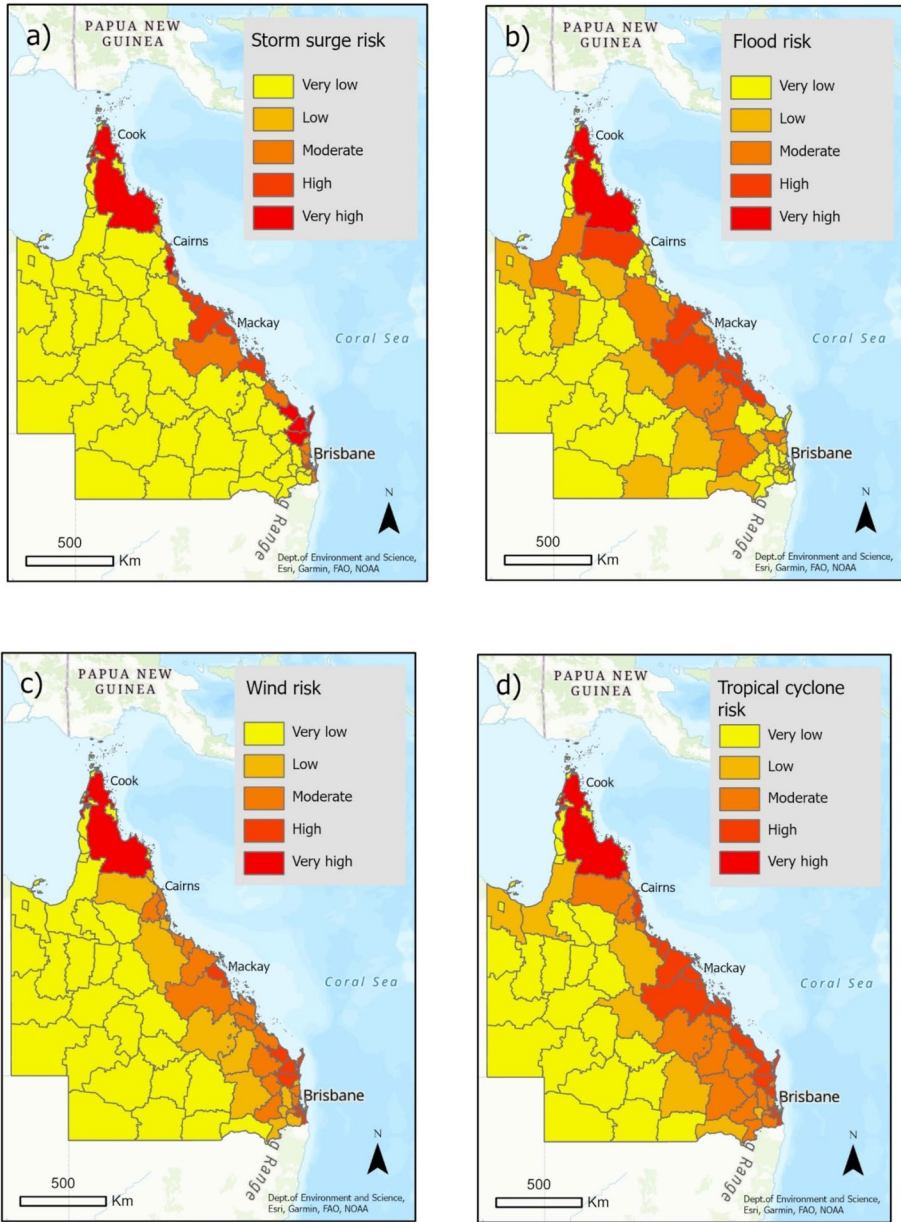


Fig. 8 Maps of TC Risk for QLD LGAs: **a** storm surges, **b** floods, **c** winds, and **d** a combined TC Risk map produced by averaging risk from all three hazards

reviews, assessment of LGA’s specific risk classifications, e.g., quantification of risk, is difficult. Mapping TC risk, we classed it from very low (0) to very high (1); however, quantifying what each class means in terms of damage or impact was out of the scope of this study. Additionally, the same class is not equal across hazards. For example,

moderate risk in the storm surge map may not equal the same risk in terms of damage or impact for wind risk. This is due to the natural breaks classification method which automatically distributes classes for each set of data (Stefanidis and Stathis 2013). As the data values of storm surge risk across all 78 LGAs are different and differently distributed compared to wind risk, natural breaks will have created classes with different boundaries. Of note is that even if boundaries were the same, in the case of TCs, storm surge, flooding and winds still damages communities and the environment differently. While further validation and quantification will be required to determine if a very low risk LGA is truly safe, the developed risk maps provide comparative analysis of risk distribution across the state and identify QLD LGAs which are at higher TC risk.

4 Conclusions

TC risk assessment and mapping for Queensland, Australia considering the multiple hazards of storm surge, flooding, and wind has been conducted in this study. In addition to TC hazards, exposure and vulnerability of QLD population, infrastructure, and the natural environment to TCs were considered.

TC multi-hazard risk maps were produced at the Local Government Area level combining layers of exposure, vulnerability, and hazards in ArcGIS, and regions with higher risk of being impacted by TCs were identified. It was found that for all three hazards, risk was higher along the state's eastern coast, particularly in LGAs of Cook Shire, Mackay Regional and Fraser Coast Regional and surroundings.

This study was primarily limited by the data used. Only global hazard datasets were available which meant finer scale features in QLD topography, bathymetry and floodplains could not be captured. Exposure and vulnerability indicators were chosen to ensure aspects of population, infrastructure and the environment were considered, however, this may have led to less robust indicators being used. Simple methodologies and calculations including equal weighting of indicators and normalisation of raw data also contributed to certain limitations of the presented risk assessment.

Further work should look to source higher resolution, more region-specific hazard data, as well as more robust exposure and vulnerability indicators. Validation and quantification studies of the calculated risk values would serve to improve the refinement and application of the developed methodology, and expansion to the entire Australian region.

Despite the limitations, this study achieved its aim of developing a reproducible methodology for TC multi-hazard risk assessment and mapping. By including exposure and vulnerability indicators from aspects of human population, infrastructure, and the environment, as well as considering the multi-hazard nature of TCs, this study contributes to advancing methodology of risk assessments, one of the key components of proactive disaster management.

While the methodology developed in this study is tailored to QLD, this research ultimately serves as a successful proof of concept for the TC risk assessment and mapping and could be extended to other regions of Australia as well as other countries at risk of TC impacts.



Fig. 9 Map of Queensland with named Local Government Areas as of March 15, 2008 (Stronger Councils, CC BY-SA 3.0 AU)

Appendix

See Fig. 9.

Acknowledgements "Climate Change and Southern Hemisphere Tropical Cyclones" International Initiative provided tropical cyclone best track data. Authors express sincere gratitude to colleagues from the Climate

Risk and Early Warning Systems (CREWS) team at the Australian Bureau of Meteorology and Monash University for their helpful advice and guidance.

Funding The authors have not disclosed any funding.

Declarations

Conflict of interest The authors declare no conflict of interest.

References

- Aguirre-Ayerbe I, Martínez Sánchez J, Aniel-Quiroga Í, González-Riancho P, Merino M, Al-Yahyai S, Medina R (2018) From tsunami risk assessment to disaster risk reduction – the case of Oman. *Natural Hazards and Earth Syst Sci* 18(8):2241–2260
- Ahmed I (2020). An assessment-based toolkit for management of urban disasters. In: An interdisciplinary approach for disaster resilience and sustainability (pp. 497–519).
- Amadio M, Mysiak J, Marzi S (2019) Mapping socioeconomic exposure for flood risk assessment in Italy. *Risk Anal* 39(4):829–845. <https://doi.org/10.1111/risa.13212>
- Anderson GB, Ferreri J, Al-Hamdan M, Crosson W, Schumacher A, Guikema S, Peng RD (2020) Assessing United States county-level exposure for research on tropical cyclones and human health. *Environ Health Perspect* 128(10):107009. <https://doi.org/10.1289/EHP6976>
- Arthur WC (2021) A statistical-parametric model of tropical cyclones for hazard assessment. *Nat Hazard* 21(3):893–916. <https://doi.org/10.5194/nhess-21-893-2021>
- Beck MW, Losada IJ, Menendez P, Reguero BG, Diaz-Simal P, Fernandez F (2018) The global flood protection savings provided by coral reefs. *Nat Commun* 9(1):2186. <https://doi.org/10.1038/s41467-018-04568-z>
- Bhardwaj J, Asghari A, Aitkenhead I, Jackson M, Kuleshov Y (2021) Climate risk and early warning systems adaptation strategies for the most vulnerable communities. *J Sci Policy Gov.* <https://doi.org/10.38126/jspg180201>
- BNHCRRC (2020) Australian disaster resilience index. <https://www.bnhcrc.com.au/resources/adri-reports> accessed 09/01/2023
- Den Boer L (2011) Normalized ArcTan S-Function - a versatile smoothing function
- Bureau of Meteorology (2020). Australian tropical cyclone outlook for 2020 to 2021. <http://www.bom.gov.au/climate/cyclones/australia/archive/20201012.archive.shtml> accessed 09/01/2023
- Cardona O-D, Ordaz MG, Mora MG, Salgado-Gálvez MA, Bernal GA, Zuloaga-Romero D, González D (2014) Global risk assessment: A fully probabilistic seismic and tropical cyclone wind risk assessment. *Int J Dis Risk Reduct* 10:461–476. <https://doi.org/10.1016/j.ijdr.2014.05.006>
- Churchill, J., Taylor, D., Burston, J. M., & Dent, J. (2017) Assessing storm tide hazard for the north-west coast of Australia using an integrated high-resolution model system
- Colette A, Leith N, Daniel V, Bellone E, Nolan DS (2010) Using mesoscale simulations to train statistical models of tropical cyclone intensity over land. *Monthly Weather Rev* 138(6):2058–2069
- Crichton D (1999) The risk triangle. *natural disaster management*, pp. 102–103
- Cyclone Debbie (2017): https://en.wikipedia.org/wiki/Cyclone_Debbie accessed 17/07/2021
- Didier D, Baudry J, Bernatchez P, Dumont D, Sadegh M, Bismuth E, Sévigny C (2018) Multihazard simulation for coastal flood mapping Bathub versus numerical modelling in an open estuary Eastern Canada. *J Flood Risk Manag.* <https://doi.org/10.1111/jfr3.12505>
- Do C, Saunders GE, Kuleshov Y (2022) Assessment of tropical cyclone risk to coral reefs: case study for Australia. *Remote Sensing* 14(23):6150. <https://doi.org/10.3390/rs14236150>
- Downing TE, Butterfield R, Cohen S, Huq S, Moss R, Rahman A, Sokona Y, Stephen L (2001) Vulnerability indices: climate change impacts and adaptation. *UNEP Policy Series*, UNEP.
- Dube SK, Murty TS, Feyen JC, Cabrera R, Harper BA, Bales JD, Amer S (2010) Storm surge modeling and applications in coastal areas. In *Global perspectives on tropical cyclones* (pp. 363–406)
- GAR Atlas Risk Data Platform. <https://risk.preventionweb.net/>. Accessed 09 Jan 2023
- Garcia C, Fearnley CJ (2012) Evaluating critical links in early warning systems for natural hazards. *Environ Hazards* 11(2):123–137. <https://doi.org/10.1080/17477891.2011.609877>
- Gori A, Lin N, Xi D (2020) Tropical cyclone compound flood hazard assessment: from investigating drivers to quantifying extreme water levels. *Earth's Future.* <https://doi.org/10.1029/2020ef001660>

- Gray WM (1998) The formation of tropical cyclones. *Meteorol Atmos Phys* 67(1):37–69. <https://doi.org/10.1007/BF01277501>
- Haynes K, Coates L, van den Honert R, Gissing A, Bird D, Dimer de Oliveira F, Radford D (2017) Exploring the circumstances surrounding flood fatalities in Australia—1900–2015 and the implications for policy and practice. *Environ Sci Policy* 76:165–176. <https://doi.org/10.1016/j.envsci.2017.07.003>
- Hoque MA-A, Phinn S, Roelfsema C, Childs I (2017) Modelling tropical cyclone risks for present and future climate change scenarios using geospatial techniques. *Int J Digital Earth* 11(3):246–263. <https://doi.org/10.1080/17538947.2017.1320595>
- Hsu SA, Yan Z (1998) A note on the radius of maximum wind for hurricanes.
- Kuleshov Y, Qi L, Fawcett R, Jones D (2008) On tropical cyclone activity in the Southern Hemisphere: trends and the ENSO connection. *Geophys Res Lett.* <https://doi.org/10.1029/2007gl032983>
- Kuleshov Y, Chané Ming F, Qi L, Chouaibou I, Hoareau C, Roux F (2009) Tropical cyclone genesis in the Southern Hemisphere and its relationship with the ENSO. *Ann Geophys* 27(6):2523–2538. <https://doi.org/10.5194/angeo-27-2523-2009>
- Kuleshov Y, Fawcett R, Qi L, Trewin B, Jones D, McBride J, Ramsay H (2010) Trends in tropical cyclones in the South Indian Ocean and the South Pacific Ocean. *J Geophys Res.* <https://doi.org/10.1029/2009jd012372>
- Kuleshov Y, Gregory P, Watkins AB, Fawcett RJB (2020) Tropical cyclone early warnings for the regions of the Southern Hemisphere: strengthening resilience to tropical cyclones in small island developing states and least developed countries. *Nat Hazards* 104(2):1295–1313. <https://doi.org/10.1007/s11069-020-04214-2>
- Lavender SL, McBride JL (2020) Global climatology of rainfall rates and lifetime accumulated rainfall in tropical cyclones: influence of cyclone basin, cyclone intensity and cyclone size. *Int J Climatol.* <https://doi.org/10.1002/joc.6763>
- Lee C-Y, Tippet MK, Sobel AH, Camargo SJ (2018) An Environmentally forced tropical cyclone hazard model. doi: <https://doi.org/10.1002/Received>
- Mendelsohn R, Zheng L (2020) Coastal resilience against storm surge from tropical cyclones. *Atmosphere.* <https://doi.org/10.3390/atmos11070725>
- Mohanty UC, Gupta A (1997) Deterministic methods for prediction of tropical cyclone tracks. *Mausam* 48(2):257–272
- Mortlock TR, Metters D, Soderholm J, Maher J, Lee SB, Boughton G, Goodwin ID (2018) Extreme water levels, waves and coastal impacts during a severe tropical cyclone in northeastern Australia: a case study for cross-sector data sharing. *Natural Hazards and Earth Syst Sci* 18(9):2603–2623
- Moskaitis JR (2008) A case study of deterministic forecast verification: tropical cyclone intensity. *Weather Forecast* 23(6):1195–1220. <https://doi.org/10.1175/2008waf2222133.1>
- Muis S, Verlaan M, Winsemius HC, Aerts JC, Ward PJ (2016) A global reanalysis of storm surges and extreme sea levels. *Nat Commun* 7:11969. <https://doi.org/10.1038/ncomms11969>
- National Research Council. (1991) Hazard and risk assessment. a safer future: reducing the impacts of natural disasters, 2.
- Ntajal J, Lamptey B, Mianikposogbedji J (2016) Flood vulnerability mapping in the lower mono river basin in Togo, West Africa.
- Paerl HW, Hall NS, Hounshell AG, Rossignol KL, Barnard MA, Luettich RA, Harding LW (2020) Recent increases of rainfall and flooding from tropical cyclones (TCs) in North Carolina (USA): implications for organic matter and nutrient cycling in coastal watersheds. *Biogeochemistry* 150(2):197–216. <https://doi.org/10.1007/s10533-020-00693-4>
- Plotkin DA, Webber RJ, O'Neill ME, Weare J, Abbot DS (2019) Maximizing simulated tropical cyclone intensity with action minimization. *J Adv Model Earth Syst* 11(4):863–891. <https://doi.org/10.1029/2018ms001419>
- Puotinen M, Drost E, Lowe R, Depczynski M, Radford B, Heyward A, Gilmour J (2020) Towards modelling the future risk of cyclone wave damage to the world's coral reefs. *Glob Change Biol* 26(8):4302–4315. <https://doi.org/10.1111/gcb.15136>
- Qian G, Chen L, Kuleshov Y (2022) Improving methodology for tropical cyclone seasonal forecasting in the Australian and the South Pacific Ocean regions by selecting and averaging models via metropolis-gibbs sampling. *Remote Sens* 14(22):5872. <https://doi.org/10.3390/rs14225872>
- Rolfe MI, Pit SW, McKenzie JW, Longman J, Matthews V, Bailie R, Morgan GG (2020) Social vulnerability in a high-risk flood-affected rural region of NSW. *Aus Natural Hazards* 101(3):631–650. <https://doi.org/10.1007/s11069-020-03887-z>
- Ryan CJ (1993) Costs and benefits of tropical cyclones, severe thunderstorms and bushfires in Australia. *Clim Change* 25(3–4):353–367. <https://doi.org/10.1007/bf01098381>

- Rygel L, O'sullivan D, Yarnal B (2006) A method for constructing a social vulnerability index: an application to hurricane storm surges in a developed country. *Mitig Adapt Strat Glob Change* 11(3):741–764. <https://doi.org/10.1007/s11027-006-0265-6>
- Sahana M, Hong H, Ahmed R, Patel PP, Bhakat P, Sajjad H (2019) Assessing coastal island vulnerability in the Sundarban biosphere reserve, India, using geospatial technology. *Environ Earth Sci*. <https://doi.org/10.1007/s12665-019-8293-1>
- Sahoo B, Bhaskaran PK (2018) Multi-hazard risk assessment of coastal vulnerability from tropical cyclones - A GIS based approach for the Odisha coast. *J Environ Manage* 206:1166–1178. <https://doi.org/10.1016/j.jenvman.2017.10.075>
- Stefanidis S, Stathis D (2013) Assessment of flood hazard based on natural and anthropogenic factors using analytic hierarchy process (AHP). *Nat Hazards* 68(2):569–585. <https://doi.org/10.1007/s11069-013-0639-5>
- Structural design actions Part 2: Wind actions. (2011). AS/NZS 1170.2:2011: Standards Australia
- Touma D, Stevenson S, Camargo SJ, Horton DE, Diffenbaugh NS (2019) Variations in the intensity and spatial extent of tropical cyclone precipitation. *Geophys Res Lett* 46(23):13992–14002. <https://doi.org/10.1029/2019gl083452>
- Volpi E, Fiori A, Grimaldi S, Lombardo F, Koutsoyiannis D (2015) One hundred years of return period: strengths and limitations. *Water Resour Res* 51(10):8570–8585. <https://doi.org/10.1002/2015wr017820>
- Wijnands J, Qian G, Shelton K, Fawcett RJB, Chan J, Kuleshov Y (2015) Seasonal forecasting of tropical cyclone activity in the Australian and the South Pacific Ocean regions. *Math Clim Weather Forecast*. <https://doi.org/10.1515/mcwf-2015-0002>
- Wijnands JS, Qian G, Kuleshov Y (2016) Spline-based modelling of near-surface wind speeds in tropical cyclones. *Appl Math Model* 40(19):8685–8707. <https://doi.org/10.1016/j.apm.2016.05.013>
- Wilson A, Fitzgerald GJ, Mahon S (2010) Hospital beds: a primer for counting and comparing. *Med J Aust* 193(5):302–304. <https://doi.org/10.5694/j.1326-5377.2010.tb03913.x>
- World Meteorological Organisation (2021) Tropical Cyclones. <https://public.wmo.int/en/our-mandate/focus-areas/natural-hazards-and-disaster-risk-reduction/tropical-cyclones> accessed 09/01/2023
- Zhang K, Xiao C, Shen J (2008) Comparison of the CEST and SLOSH models for storm surge flooding. *J Coastal Res* 242:489–499. <https://doi.org/10.2112/06-0709.1>

Publisher's Note Springer Nature remains neutral with regard to jurisdictional claims in published maps and institutional affiliations.